18TH WORLD CONFERENCE ON EARTHQUAKE ENGINEERING
WCEE2024
MILAN

MILAN, ITALY
30TH JUNE - 5TH JULY 2024

www.wcee2024.it

SEISMIC RISK SENSITIVITY ANALYSIS OF A LARGE DRINKING WATER DISTRIBUTION NETWORK IN CENTRAL CHILE

J.P Muñoz[1], J.C. de la Llera[2,3], S. Castro, Y. Alberto[2], A. Poulos, F. Arróspide

[1] Research Center for Integrated Disaster Risk Management (CIGIDEN) ANID/FONDAP/1523A0009, Santiago, Chile, jpmunoz4@uc.cl

[2] Research Center for Integrated Disaster Risk Management (CIGIDEN) ANID/FONDAP/1523A0009, Santiago, Chile

[3] Department of Structural and Geotechnical Engineering, Pontifical Catholic University of Chile, Santiago, Chile

Abstract: *The correct functioning of cities depends on a series of complex networks that are critical for operation, given the direct and indirect negative impacts on the population caused by any service disruption. One the most critical lifelines is the Drinking Water Distribution Network (DWDN), whose malfunctioning after an earthquake may have important sanitary consequences at the individual level, but also due to the impact on other critical infrastructure such as hospitals, which may not be able to provide healthcare services when they are most needed. Seismic risk assessment of DWDNs may be used to identify critical elements, rank components, and propose mitigation strategies. While the criticality of surfaced elements, such as tanks, is evident given their small number, the effect of buried elements (pipes) damage is less visible, especially if they are distant from tanks. Correctly assessing the implications of pipe damage in large DWDN is difficult given the large system's redundancy, and the thousands of kilometers of pipes of different materials and diameters buried under a city on very different soil conditions. Consequently, a detailed model of the DWDN that identifies possible seismic damage on network pipes and performance consequences is a useful tool. This research describes such a hydraulic model built in EPANET for the DWDN of a large conurbation in central Chile formed by the cities of Valparaiso, Viña del Mar, and Concon. Seismic risk assessment is performed using Peak Ground Velocity for the ground motion intensity measure, three repair rate models to represent seismic vulnerability of pipes, and two damage-state models. A hydraulic analysis was carried out to assess the earthquake performance of the damaged network in terms of the Unsupplied Water Demand (UWD) to the population, for the entire conurbation and for the hospitals in the zone under study. Results of the model showed significant dispersion, hence, a sensitivity analysis of the risk results was carried out by weighting the different vulnerability models, changing the vulnerability factors due to system properties such as pipe material, soil liquefaction potential, and the threshold values of the parameters of the different damage-state models. It is concluded that risk results exhibit large sensitivity to the different modelling assumptions. Results also show that the water service is highly non-linear and it is shut down completely if pipe damage reaches about 30% of the network.*

1. Introduction

The risk of service interruption in water distribution systems located in seismic-prone zones must be assessed and managed to maintain an adequate performance during and after a seismic event. This is particularly important in modern cities because an interruption of the service has direct and indirect negative impacts on the population and also affects other interdependent lifelines. Assessing seismic risk in an efficient, methodic and thorough way is a difficult task, because a Drinking Water Distribution Network (DWDN) is a large and complex system, with high redundancy and thousands of kilometers of pipes of different materials and diameters buried on different soil conditions, along with several other components, such as tanks, valves and

pumps. A detailed model of the DWDN under study is required to achieve the goal of understanding its seismic behavior and proposing mitigation strategies. Seismic damage in DWDN has been studied in the past (e.g. (Choi and Kang, 2020; Cimellaro et al., 2016; Hamamoto et al., 2021; Yoon et al., 2021)) usually focusing on pipe damage, given that they outnumber other elements in the system. Pipelines are subjected to wave propagation and soil deformation, which requires appropriate estimations of peak ground velocity (PGV) for the former and permanent ground deformation (PGD) for the latter, since it has been shown that PGV is related to ground strain, whereas PGD is associated with various pipe failure modes (American Lifelines Association, 2001; Xu et al., 2021). For instance, liquefaction-induced deformation, that can produce lateral displacement and post-liquefaction settlement, among other phenomena, has caused significant damage in previous earthquakes (Alberto et al., 2022). While ground deformation creates more severe damage, it is concentrated in small areas, whereas wave propagation is an extensive phenomenon. With that in mind, this paper will focus on the effect of wave propagation (i.e., PGV) to propose a probabilistic framework for estimating seismic risk in a DWDN, applied to the cities of Valparaiso, Viña del Mar and Concón, a conurbation in the central coast of Chile. A probabilistic seismic hazard analysis will be carried out to simulate consistent maps of PGV, and seismic damage of pipelines will be estimated combining three different Repair Rate (RR) models to account for pipe seismic vulnerability, and two models to sample the damage state of a pipe (leak or break) given its Repair Rate. Results will be processed to obtain seismic risk curves of the Unsupplied Demand of the complete network, and a sensitivity analysis will be carried out to quantify the effect of changing modelling considerations.

2. Network model construction

The DWDN of Valparaíso, Viña del Mar and Concón was modelled in the EPANET software (US EPA, 2014) because of its simplicity, widespread use and open-source nature. EPANET models consider a set of basic components such as junctions, pipes, valves, reservoirs and tanks, which are defined based on available data of the network. EPANET allows the user to implement advanced water network elements such as pumps, time patterns, water quality features, etc., however, due to the limited amount of available information for the authors, many assumptions and simplifications were undertaken. In the next paragraphs, the overall process of modelling the real-life water network elements into EPANET will be described.

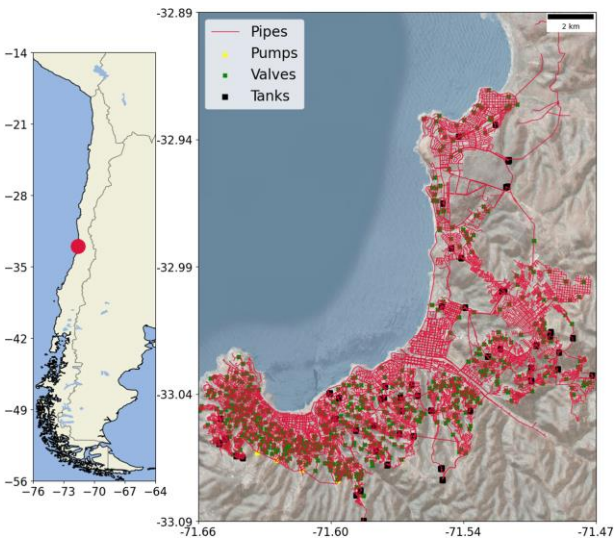

Figure 1: Drinking water distribution network of Valparaíso, Viña del Mar and Concón conurbation.

2.1. Software and raw data sources used in network modelling

Data necessary to build the EPANET model was provided by ESVAL, the private company that currently serves the conurbation under study. The supplied dataset includes GIS shape files with points representing the water tanks and valves, and polylines representing the pipes (Fig. 1). These elements were included in EPANET using the [TANKS], [VALVES] and [PIPES] objects respectively. The vertices from the pipes' polylines

shapefile were used as the EPANET object [NODES], which are required to input the water demand values in them.

Shapefile attributes include (among the most important): tank elevation, pipe diameter, pipe material, pump head, and valve diameter. Table 1 shows a summary of the available raw data. Water demand data was included as yearly average flow registered by ESVAL flowmeters, whose locations were available; however, since they did not match the pipe polylines, it was impossible to directly assign demand values to the network. To address this issue, a Python script was implemented to assign a flowmeter demand to the closest pipe polyline vertex. Most of the water supply comes from tanks located over elevated terrain, which allows gravity to transport water to the lower sectors. However, there are many tanks located in low terrain that need pumps to provide water to the inhabitants of the city. ESVAL data includes the location, head and power for each pumping station, but no pump operation curve, which is ideally required in EPANET for a proper pump representation in the model. Hence, we simplified our model by taking the head data from the pumping stations and added them to the elevation data of their associated tanks. This simplification implies that all the water pumping regime is constant, or in other words, a steady-state pumping

Table 1: Summary of the raw available data, format and attributes

Component	File	Main attributes
Tanks	Shapefile (.shp)	Latitude, longitude, elevation, min./max. levels
Pipes	Shapefile (.shp)	Latitude, longitude, diameter, material
Valves	Shapefile (.shp)	Latitude, longitude, diameter, pressure, setting
Demand	MS Excel spreadsheet (.xlsx)	Latitude, longitude, monthly volume

2.2. Model components setup and settings

All components described in the previous section were integrated using Python 3.7 scripts. The tanks' shapefile was not connected to the pipes' shapefile; therefore, we connected them manually by creating additional pipes whose attributes were defined as the same attributes from the connecting end. Pipes and valves are all considered to be in "good condition" and have no previous deterioration. In reality, pipes can be up to 50 years old, but for the sake of simplicity and availability of data, this aspect will not be considered. All [PIPES] objects are created given an "OPEN" state. Once the EPANET model was created, the hydraulic simulation was run, and an iterative process was applied to correct the orientation of the valves, until the pressure values in the pipes were in the acceptable range defined by ESVAL (Figure 2a).

3. Seismic Hazard

The seismic hazard of the region under study was characterized using 50,000 earthquake scenarios generated using the recurrence model developed for Chilean seismicity (Poulos et al., 2019), which consists of interface and intraslab seismic sources associated with the subduction of the Nazca Plate under the South American Plate. All sampled earthquakes had magnitude $M_w \geq 5$, and importance sampling (Jayaram and Baker, 2010) was used to increase the proportion of high impact earthquake scenarios by considering a uniform distribution of earthquake magnitudes, instead of the true underlying probability distribution of magnitudes (i.e., a mixture of truncated exponential distributions). Moreover, only the seismic sources close to the cities were considered, and the hypocentre of each earthquake realization was sampled assuming a uniform distribution inside each seismic source. Once magnitudes and hypocentres were obtained, PGV maps were generated for each network component using the ground motion model (GMM) developed by Parker (Parker et al., 2022) and considering the regional adjustment factors for South America. The rupture distances (i.e., the closest distances from the sites to the rupture surface), which is required by the GMM to estimate PGVs, were computed using the source scaling relations developed by Strasser (Strasser et al., 2010). Moreover, the spatial correlation of PGV was also considered by using the model developed by Goda (Goda and Atkinson, 2010), which only depends on the distances between sites. It is well known (Kwong and Jaiswal, 2023) that pipe seismic damage is related to both ground shaking (e.g., PGV) and ground failure (e.g., landslides,

liquefaction), however, only the former was considered in this study, because it affects larger areas, and because including the ground failure requires adequate models that are consistent with the ground shaking model. Such models are currently unavailable for the area under study, but are under development and will be included in a future journal publication.

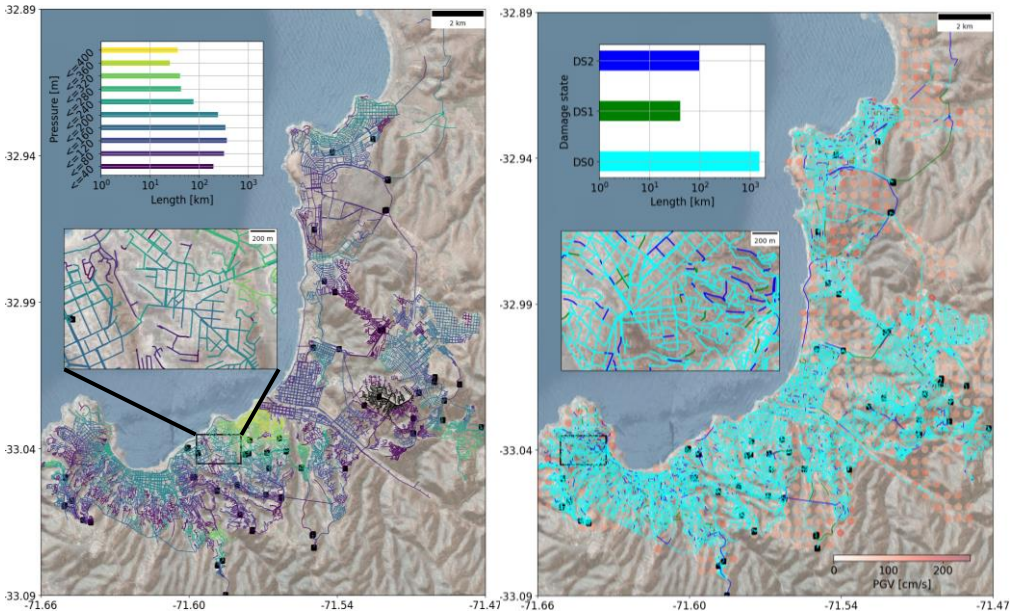

Figure 2: Left: pressure distribution in the undamaged network. Right: damaged scenario for one realization with unsupplied water demand of 70%, showing undamaged (cyan), leaking (green) and broken (blue) pipes.

4. Pipe vulnerability

One of the possible goals of risk assessment is to identify critical network components, in order to determine adequate mitigation strategies to guarantee normal network functionality. Clearly, tanks and pumps are critical elements, due to their role and reduced number. However, it is not straightforward to establish the same for pipes. With this in mind, it is possible to study pipe importance by assuming only them might be damaged when subject to an earthquake, because this would isolate the effect of pipe damage on the network functionality. Pipe damage is modeled with vulnerability functions that represent the Repair Rate (RR) of an element after a seismic event, which is the average number of failures per unit of length. This is a function of Peak Ground Velocity (PGV), Permanent Ground Deformation (PGD), and pipe properties. Given a failure, two possible damage states are defined for a pipe, leak and break. Most studies consider the assumption that when a pipe is damaged due to PGV, 80% of the time this corresponds to leaks and 20% to breaks, while the percentages are reversed when damage is due to PGD (American Lifelines Association, 2001). Since there are no models to estimate PGD in the zone under study, this research considered only PGV to compute the Repair Rate. This was carried out with three different models from the literature, that were combined into one RR estimation.

The first RR model was proposed by ALA (American Lifelines Association, 2001)

$$RR_{ALA} = 0.00126\, K_1\, PGV^{1.173} + \epsilon \quad (1)$$

$$K_1 = K_m \cdot K_d \quad (2)$$

, where RR is in [rep/km]; PGV is in [cm/s]; K_1 is a correction factor that considers pipe material (K_m) and diameter (K_d); and ϵ is the regression residual. This model is based on 18 earthquakes from the Americas and Japan, including Kobe, Loma Prieta and Mexico City.

The second model was developed for Japan (Isoyama et al., 2000)

$$RR_{ISO} = 3.11 \times 10^{-3}\, C\, (PGV - 15)^{1.30} + \epsilon \quad (3)$$

$$C = C_m\, C_d\, C_t\, C_l \quad (4)$$

, where RR is in [rep/km]; PGV is in [cm/s]; C is a correction factor that considers pipe material (C_m), diameter (C_d), topography (C_t), and liquefaction potential (C_l); and ϵ is the regression residual. This model is based on the damage caused by the Kobe earthquake (1995) to the Ashiya and Ishinomiya cities.

The third model was developed for New Zealand (Bellagamba et al., 2019):

$$\ln RR_{Bel} = f_0(PGV) + \sum_{i=1}^{n} C_i(h_i) + \epsilon = a + b\ PGV + a_0\ PGV^{b_0} + \epsilon \quad (5)$$

, where RR is in [rep/km]; PGV is in [cm/s]. The RR value depends on PGV according to the function f_0, and a series of correction factors C_i that depend on parameters h_i. After rearranging the expression, the regression parameters a, b, a_0 and b_0 depend on the pipe performance group, material, diameter and soil cyclic resistance ratio (CRR). This model is based on the Christchurch earthquake and provides a detailed quantification of uncertainty ϵ.

For each pipe, the PGV was computed as the average of its end nodes, and this value was used to compute the Repair Rate according to equations (1) to (5). Then, the predictions of the three models were combined using equal weights for the base case, and other weight values for the sensitivity analysis presented in a following section. Once a RR value was computed for a pipe, the total number of failures was sampled from a Poisson distribution:

$$f(x, \lambda) = P(X = n) = \frac{\lambda^n e^{-\lambda}}{n!} \quad (6)$$

, where the Poisson distribution parameter, $\lambda = RR \cdot L$, is the expected number of failures of a pipe with length L and RR expected repairs per unit of length; and n is the total number of failures, considering leaks and breaks, $n = n_{breaks} + n_{leaks}$. As expected, longer pipes should have on average more failures, given the same RR. As it was mentioned before, most studies use the ALA (American Lifelines Association, 2001) and HAZUS (FEMA, 1997) assumption to determine n_{breaks} and n_{leaks}. Thus, given a pipe, one may obtain a PGV value from the seismic hazard map, compute the associated RR value with Equations (1) to (5), sample n from Equation (6), and then sample the nature of each failure considering that 80% of them are leaks. The major drawback of this assumption is that the proportion of breaks and leaks is independent of the PGV level, which is not realistic, since it is expected that for very low PGV values all failures should correspond to leaks, whereas for very high PGV values all failures should be breaks. To take this into consideration, a more realistic model may be proposed, making the proportion of leaks and breaks a function of PGV. In particular for this study, based on results obtained from elsewhere (Lanzano et al., 2014), it was considered that for PGV < 45 cm/s all failures are leaks, while for PGV > 95 cm/s failures correspond to breaks only. For intermediate PGV values, the probability of a break may be obtained by linearly interpolating between these points.

5. Hydraulic model with damage

Once pipe damage has been determined by following the procedure of the previous section, the next step was to model it in the hydraulic model. On one hand, a leakage was represented with the [EMITTERS] object in EPANET, which is an optional component associated to a junction that produces a water loss as a function of the pressure. The water flow through an emitter is computed in EPANET with a generalized form of the Torricelli equation that characterizes flow through a hole in a tank, as in Equation (7), where the water flow Q is a function of the junction pressure H, the emitter exponent n, and the flow coefficient C, which in turn is a function of the cross-section area of the hole A, the gravity acceleration g, and the discharge coefficient $C_d < 1$, that depends on energy losses due to turbulence. In EPANET, C can be defined individually for each emitter, while n is defined globally for the whole model.

$$Q = \underbrace{C_d A (2g)^n}_{C} H^n = C H^n \quad (7)$$

Therefore, an emitter may be completely characterized by selecting an emitter exponent n, a hole cross-section area A, and a discharge coefficient C_d. Please, notice that both A and C_d are random variables because holes may vary in size, while energy losses depend on different variables, such as hole aspect ratio. If a pipe has multiple leaks, they are all randomly generated and then combined into one equivalent emitter by summing their flow coefficients C. Based on previous studies (Klise et al., 2017; Yoo et al., 2016), the hole

cross-section area is assumed to follow an uniform distribution, as a function of the pipe cross-section area, A_0

$$A \sim U(0.05A_0, 0.10A_0) \tag{8}$$

Similarly, the discharge coefficient C_d is assumed to follow a normal distribution as a function of the head pressure H, in meters of water column (Schwaller et al., 2015):

$$C_d \sim \begin{cases} 0.5 & , H < 20 \\ N(0.575, 0.026) & , 20 \leq H < 30 \\ N(0.650, 0.030) & , 30 \leq H < 45 \\ N(0.725, 0.035) & , 45 \leq H < 60 \\ N(0.800, 0.039) & , 60 \leq H \end{cases} \tag{9}$$

On the other hand, pipe break was modeled by modifying the network by: (i) removing the pipe; (ii) replacing it with two half-pipes that go from the pipe end nodes to the midpoint of the original pipe, where its height is linearly interpolated from the heights of the end nodes; (iii) adding an empty reservoir to both free ends of the new half-pipes (i.e., reservoir's head is equal to its height); and (iv) adding a check-valve on both half-pipes, so water can only flow into the reservoirs and not from them. By following this procedure, the broken pipe disconnects parts of the network and allows for considerable water and pressure losses. Whenever a pipe experiences both leaks and breaks, only the latter is modeled, because the water and pressure losses of the former are negligible in comparison. Additionally, at most one break is modeled for each pipe, because any following break will have no effect on the network.

Having modeled a damaged DWDN, like the one shown in Figure 2b, a pressure-driven hydraulic simulation was carried out in EPANET. The performance of the network was measured considering the Unsupplied Demand UD as output variable, as defined in Equation (10), where q_{D_i} is the water that is actually supplied to node i by the network, and D_i is the water demand required by node i. It may be noticed that a value of $UD = 0$ implies that the DWDN is fully operational, while $UD = 1$ means that no water is provided to the entire network.

$$UD = 1 - \frac{\sum_i q_{D_i}}{\sum_i D_i} \tag{10}$$

6. Seismic risk and sensitivity analysis

A risk analysis (Jayaram and Baker, 2010; Poulos et al., 2017) was carried out considering the 50,000 seismic scenarios. For each one, the damage state of the pipes was sampled as explained before, a hydraulic simulation was run, and the Unsupplied Demand was computed. Results of UD were then combined in a risk curve, as shown in Figure 3, where the curve in orange corresponds to the results obtained when the ALA assumption for pipe breaking probability was used, while the blue curve corresponds to the PGV-dependent model being considered. It may be noticed that selected model greatly affects the results, because ALA's rule underestimates the number of pipe breaks (and therefore the UD) for seismic scenarios with large PGV values, while the opposite happens for scenarios with low PGVs. Also, Figure 3 shows that the DWDN is very robust in both cases, presumably due to its high redundancy, since high return periods are observed for the entire range of UD.

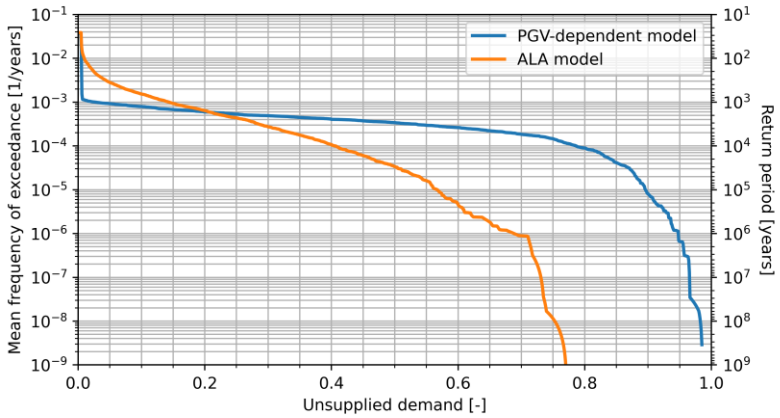

Figure 3: Risk curve of unsupplied demand considering ALA's and a PGV-dependent model for pipe breaking probability

While the risk curve of Unsupplied Demand is a useful result, additional information is required to better understand the seismic performance of the DWDN. For instance, the network is composed by tens of thousands of kilometers of pipes, thus a natural question would be how much of that total pipe length (L_{tot}) must be broken (L_{break}) for the system to reach a certain level of UD. This is illustrated in Figure 4a, that shows the PGV-dependent model results. It may be inferred that the DWDN collapses when around 20%-30% of its pipes (in terms of length) are broken, although considerable performance loss is observed for much smaller values. For instance, the UD increases rapidly and linearly until around 5% of the total pipe length is broken, where the UD may take values roughly between 55% and 80%. After that point, the behavior is more nonlinear, and the variance tends to decrease. It may be also noticed on the secondary histograms that most seismic scenarios produce small values of UD, and only a small group of them cause major losses. This is also better appreciated in Figure 4b, that shows how only scenarios with magnitude $M_w > 8$ produce values of UD greater than 10%, with a significant variability in the results.

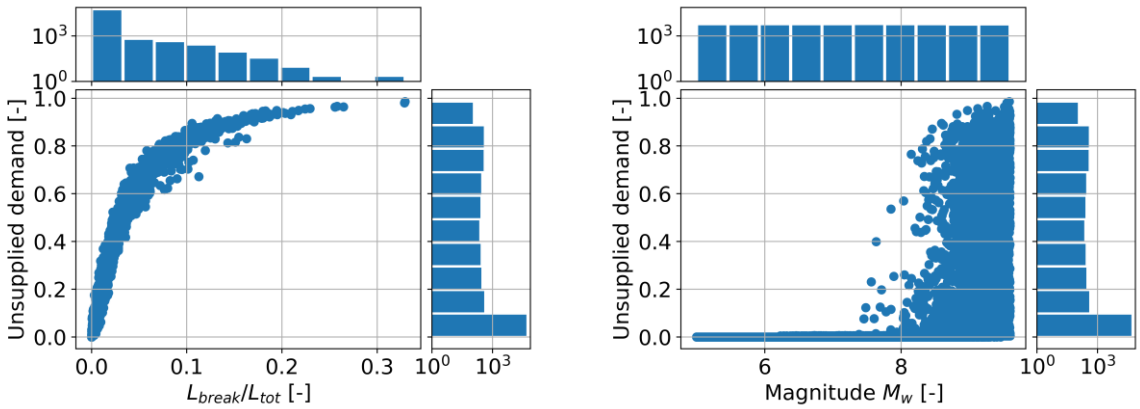

(a) (b)

Figure 4: Summary of the risk analysis with the PGV-dependent model for pipe breaking probability. Left: non-linearity of the Unsupplied Demand as a function of the total length of broken pipes. Right: damage to the network as a function of event magnitude

A sensitivity analysis was performed to study the impact of the Repair Rate model in the risk curve. Given that the PGV-dependent breaking probability model estimates more damage than ALA's model, it was considered as the base case for this section. As it was mentioned before, the three RR models of Equations (1) to (5) were combined with equal weights to estimate seismic damage for each pipe for the base case. Figure 5 compares the results of this approach and those of using only one of the three RR models. It may be noticed that the impact of the selected RR model is considerable. All curves overlap for $UD < 1\%$, and after that point the ALA

Repair Rate model consistently estimates the highest return period (i.e., less damage), while the Isoyama, Bellagamba and combined RR models continue to overlap until $UD = 70\%$. For higher UD values, the Isoyama model estimates the highest impact on the DWDN, and Bellagamba the lowest of the three, while the combined model gives approximately an average of them, as expected.

Another variable of interest for the sensitivity analysis is the pipe breaking probability, since Figures 3 and 4a suggest that it plays a critical role in the DWDN performance loss. To evaluate this effect, the complete analysis was repeated considering the combined RR models and the ALA pipe breaking probability model, with different values (i.e., 10%, $20\%, 40\%, 60\%$, 80% and 100%). Results are presented in Figure 6, along with the case of using the PGV-dependent breaking probability model. As expected, the effect of pipe breaking is considerable on the UD risk curve, because a change in the probability of ALA's model greatly affects the obtained return periods. For example, for $UD = 40\%$ the return period is approximately 600,000 years when a breaking probability of 10% is considered, while for a 100% breaking probability, the return period is roughly 950 years. It may also be observed that the PGV-dependent model overlaps with the 100% breaking probability model of ALA for $UD > 80\%$, and for lower UD values it crosses all the other curves, as a consequence of the pipe breaking probability smoothly changing from 0% to 100% in this model as the PGV increases.

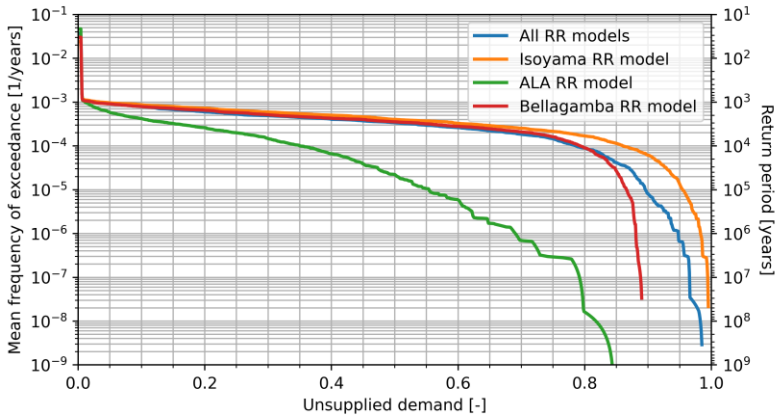

Figure 5: Effect of selecting a different Repair Rate model on the Unsupplied Demand risk curve

The obtained results suggest that further studies are required to better understand (i) which scenarios are causing more damage and why; (ii) which Repair Rate and Damage State models are adequate for the DWDN under study; and (iii) which pipes are more critical in terms of producing higher UD values when broken (i.e., the DWDN collapses when any subset that corresponds to 30% of the pipes is broken?). A detailed analysis of these points will be addressed in a journal publication that is currently under preparation, but some results on pipe criticality are presented next as an example.

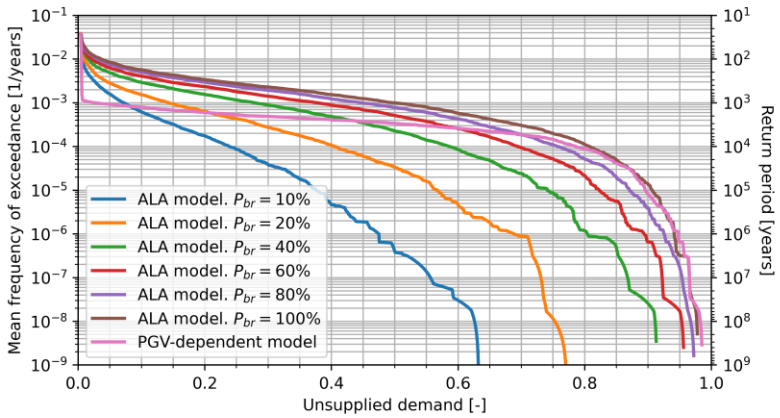

Figure 6: Effect of changing the pipe damage-state sampling model, between ALA with different threshold values, and a PGV-dependent rule

As an example of pipe criticality assessment, the DWDN was analysed considering the ALA Repair Rate and the PGV-dependent breaking probability models. Instead of focusing the assessment on a pipe-resolution level, critical zones were studied in terms of those that are more prone to suffer damage (breaks), or to have higher local UD values, as well as those that have the highest impact on the entire network UD when damaged. The motivation behind the analysis is that the provider of the drinking water distribution service may improve the network behavior by reducing the vulnerability of the pipes (e.g., replacing some of them with newer and better materials), but since there are almost 1,700 km of pipes, the investment should be focused on the most critical zones considering a practical approach (i.e., it is not practical to change a short individual pipe, but it may be possible to retrofit some blocks of the city). To illustrate the process, the DWDN was divided into five sectors using k-means clustering, as shown in Fig.7a. For each cluster, the risk curve of the fraction of broken pipes within the cluster was computed (Fig. 7b), as well as the risk curve of local UD (Fig. 7c). From these results, it is apparent that cluster 2 (aquamarine curve) is the most prone to suffer pipe breaking, however, it shows an intermediate level of importance in terms of local UD values, whereas clusters 0 (purple) and 1 (cyan) tend to be the most critical in this regard (Fig. 7c). While these results illustrate the performance of the clusters for the network as is, a sensitivity analysis of the global UD risk curve was carried out to understand the effect of local (cluster) modifications (improvements) on the complete network. As an initial approach that aims to obtain a qualitative bound for the effect of pipe improvements on the global UD risk curve, the risk analysis was computed again five times, but each time the pipes of one of the clusters were modeled as invulnerable (i.e., leaks and breaks are not allowed). The rationale behind the analysis is that if one cluster is considerably more critical than the others, then the global UD risk curve should change drastically when it is made invulnerable. Results are presented in Fig. 7d with the base case risk curve in black, and they suggest that the most critical cluster is number 0 (purple), because its risk curve go below the others, meaning that its improvement (invulnerability) is the one that reduces the probability of a level of performance loss by the highest value (i.e., it reduces the mean annual frequency of exceedance, or equivalently, increases the return period). Further studies are required to better understand the criticality in terms of different criteria, and the effect of realistic pipe improvements (e.g., pipe retrofit) on the complete DWDN performance, including a higher resolution study of critical zones (i.e., considering a higher number of clusters).

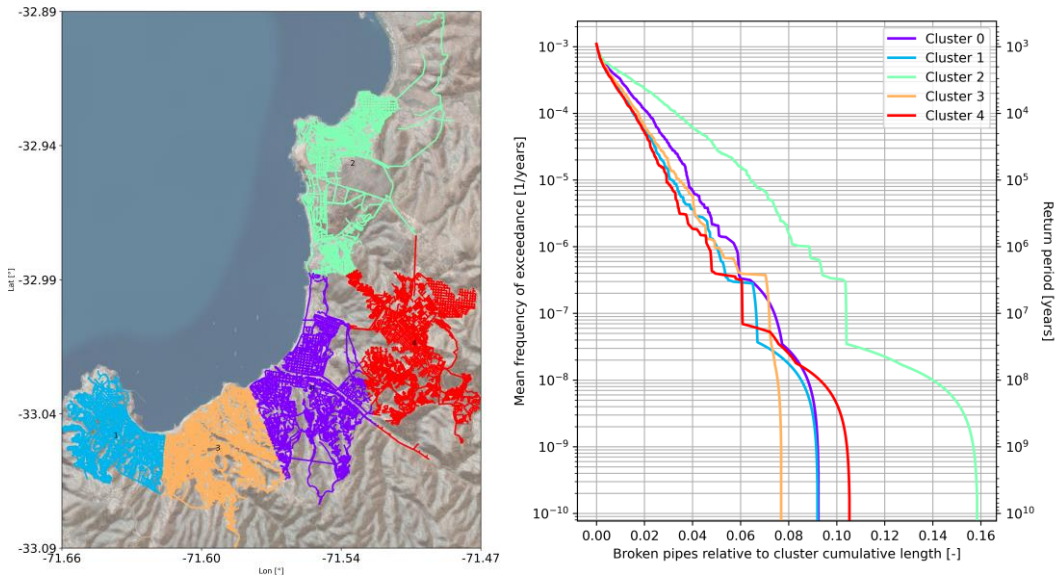

(a) (b)

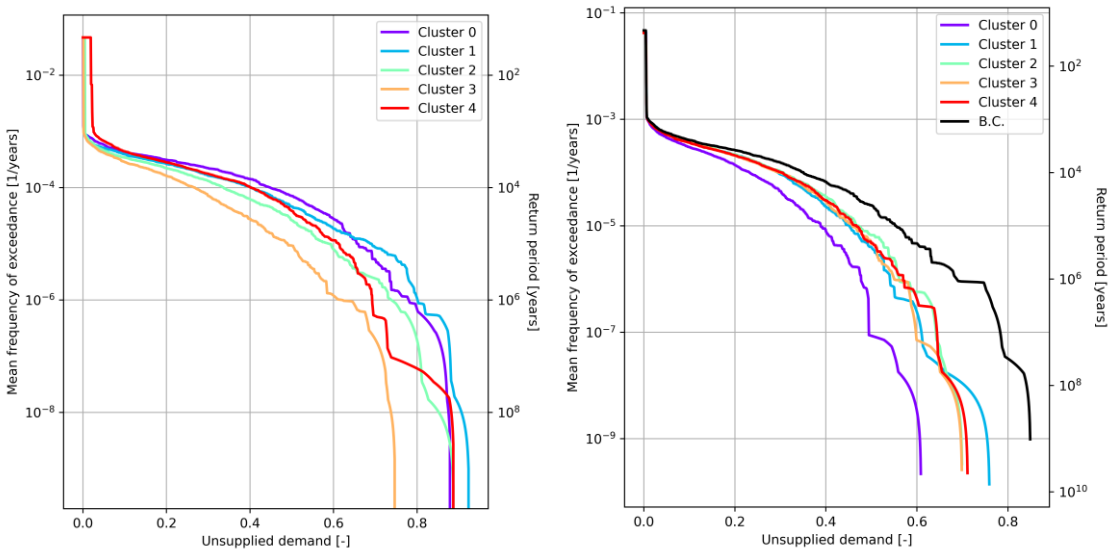

(c) (d)

Figure 7: Critical zone analysis. (a) DWDN zones obtained with k-means clustering. (b) Local risk curve of each cluster, for the fraction of broken pipes. (c) Local risk curve for each cluster, for the Unsupplied Demand. (d) Effect of cluster invulnerability on the global Unsupplied Demand risk curve.

7. Conclusions

This article presented a hydraulic model developed for the Drinking Water Distribution Network of a large conurbation in the central coast of Chile, considering the cities of Valparaíso, Viña del Mar and Concón. The model was calibrated with real data obtained from ESVAL, the private company that provides the drinking water distribution service to the conurbation; and implemented in EPANET. A seismic risk assessment was performed considering 50,000 scenarios of Peak Ground Velocity maps, generated with adequate models for the seismicity of the region. The effect of seismic damage was restricted to pipes only, to isolate the effect of their failure on the overall performance of the network and study its impact. Seismic damage was estimated using three Repair Rate models, and two pipe breaking probability models, by using a cascading sampling algorithm. Pipe seismic damage was incorporated in the hydraulic model by using emitters for the case of leakages; and with a modification of the network topology for the case of breakings, by interrupting the water flow through a broken pipe and modeling the water loss. A pressure-driven analysis was carried out in EPANET for the simulated scenarios and the Unsupplied Demand was computed for each one of them, to quantify the performance of the DWDN. Results were combined in a risk curve that suggests that (i) the DWDN is robust due to its redundancy, since high return periods were obtained; (ii) the network collapses when around 20-30% of the pipes, in terms of length, are broken; (iii) the performance of the lifeline follows a nonlinear relationship with the total length of broken pipes and event magnitude; and (iv) only a small subset of the seismic scenarios cause major performance loss on the network, although the variability is rather important. A sensitivity analysis was performed to study the importance of modelling assumptions, such as the Repair Rate model considered, and the pipe breaking probability model used. It is concluded that the effect of both aspects may not be neglected, since they produce major variations in the risk curves. For instance, changing the selected RR model may change the return period from 50,000 to 5,000 years for 40% Unsupplied Demand; whereas a variation in the pipe breaking probability in ALA's model may produce an even greater change, from 600,000 to 950 years when the value changes from 10% to 100%. Moreover, using a PGV-dependent model for estimating the pipe breaking probability, instead of ALA's rule, may have a similar impact. It was observed that the risk results of the former overlaps with the latter for $UD > 0.80$ when 100% is considered for the pipe breaking probability, while they become gradually similar to the risk results of using smaller pipe breaking probability values in ALA's model as the Unsupplied Demand becomes smaller. Additionally, a critical zone assessment of the DWDN was carried out by dividing it into five sectors using k-means clustering. The criticality was evaluated in terms of the cluster local risk curves of fraction of broken pipes and Unsupplied Demand. A sensitivity analysis was also performed to identify the most critical cluster in terms of its effect on the global

Unsupplied Demand, by recomputing the risk analysis while assuming invulnerability for the cluster under study. Cluster criticality results differ depending on the criterion considered, but both the local and global UD risk curves indicate that the central cluster is the most critical, while the northern cluster is more critical in terms of its fraction of broken pipes. Further research is needed to quantify the effect of modelling assumptions on the risk results, better understand pipe criticality and its impact on the performance loss, identify which seismic events tend to produce more damage to the network, and to better identify critical zones in the network, all of which will be addressed in a journal article currently under preparation.

8. Acknowledgements

The authors thank the National Research and Development Agency (ANID), which has financed the Projects FONDECYT 1170836 “SIBER-RISK: SImulation Based Earthquake Risk and Resilience of Interdependent Systems and Networks”, FONDECYT 1220292 “Multiscale earthquake risk mitigation of healthcare networks using seismic isolation”, and FONDEF ID22I10050 “Plataforma de simulación y evaluación del riesgo para la gestión integrada y planificación óptima de recursos críticos en redes de salud de emergencia para enfrentar condiciones extremas en la demanda hospitalaria”. Likewise, we express our gratitude to the institutions that participated and contributed to this research project, especially to the Research Center for Integrated Disaster Risk Management (CIGIDEN) ANID/FONDAP/1523A0009.

9. References

Alberto, Y., De la Llera, J.C., Aguirre, P., Monsalve, M., Molinos, M., 2022. Comparative Qualitative and Quantitative Analyses of the Seismic Performance of Water Networks during the Maule 2010, Christchurch 2010–2011, and Tohoku 2011 Earthquakes. J. Water Resour. Plann. Manage. 148, 04022004. https://doi.org/10.1061/(ASCE)WR.1943-5452.0001520

American Lifelines Association, 2001. Seismic fragility formulations for water systems.

Bellagamba, X., Bradley, B.A., Wotherspoon, L.M., Hughes, M.W., 2019. Development and Validation of Fragility Functions for Buried Pipelines Based on Canterbury Earthquake Sequence Data. Earthquake Spectra 35, 1061–1086. https://doi.org/10.1193/120917EQS253M

Choi, J., Kang, D., 2020. Improved Hydraulic Simulation of Valve Layout Effects on Post-Earthquake Restoration of a Water Distribution Network. Sustainability 12, 3492. https://doi.org/10.3390/su12083492

Cimellaro, G.P., Tinebra, A., Renschler, C., Fragiadakis, M., 2016. New Resilience Index for Urban Water Distribution Networks. J. Struct. Eng. 142, C4015014. https://doi.org/10.1061/(ASCE)ST.1943-541X.0001433

FEMA, 1997. Hazus–MH 2.1 Technical Manual. Multi-hazard Loss Estimation Methodology - Earthquake model.

Goda, K., Atkinson, G.M., 2010. Intraevent Spatial Correlation of Ground-Motion Parameters Using SK-net Data. Bulletin of the Seismological Society of America 100, 3055–3067. https://doi.org/10.1785/0120100031

Hamamoto, S., Ito, L., Tokai, A., 2021. Assessment of Renewal Priority of Water Pipeline Network against Earthquake Risk. Water 13, 572. https://doi.org/10.3390/w13040572

Isoyama, R., Ishida, E., Yune, K., Shirozu, T., 2000. Seismic damage estimation procedure for water supply piplines. Presented at the 12th World Conference on Earthquake Engineering.

Jayaram, N., Baker, J.W., 2010. Efficient sampling and data reduction techniques for probabilistic seismic lifeline risk assessment. Earthquake Engng Struct. Dyn. n/a-n/a. https://doi.org/10.1002/eqe.988

Klise, K.A., Bynum, M., Moriarty, D., Murray, R., 2017. A software framework for assessing the resilience of drinking water systems to disasters with an example earthquake case study. Environmental Modelling & Software 95, 420–431. https://doi.org/10.1016/j.envsoft.2017.06.022

Kwong, N.S., Jaiswal, K.S., 2023. A Methodology to Combine Shaking and Ground Failure Models for Forecasting Seismic Damage to Buried Pipeline Networks. Bulletin of the Seismological Society of America 113, 2574–2595. https://doi.org/10.1785/0120220132

Lanzano, G., Salzano, E., Santucci de Magistris, F., Fabbrocino, G., 2014. Seismic vulnerability of gas and liquid buried pipelines. Journal of Loss Prevention in the Process Industries 28, 72–78. https://doi.org/10.1016/j.jlp.2013.03.010

Parker, G.A., Stewart, J.P., Boore, D.M., Atkinson, G.M., Hassani, B., 2022. NGA-subduction global ground motion models with regional adjustment factors. Earthquake Spectra 38, 456–493. https://doi.org/10.1177/87552930211034889

Poulos, A., de la Llera, J.C., Mitrani-Reiser, J., 2017. Earthquake risk assessment of buildings accounting for human evacuation: EARTHQUAKE RISK ASSESSMENT OF BUILDINGS ACCOUNTING FOR EVACUATION. Earthquake Engng Struct. Dyn. 46, 561–583. https://doi.org/10.1002/eqe.2803

Poulos, A., Monsalve, M., Zamora, N., de la Llera, J.C., 2019. An Updated Recurrence Model for Chilean Subduction Seismicity and Statistical Validation of Its Poisson Nature. Bulletin of the Seismological Society of America 109, 66–74. https://doi.org/10.1785/0120170160

Schwaller, J., van Zyl, J.E., Kabaasha, A.M., 2015. Characterising the pressure-leakage response of pipe networks using the FAVAD equation. Water Supply 15, 1373–1382. https://doi.org/10.2166/ws.2015.101

Strasser, F.O., Arango, M.C., Bommer, J.J., 2010. Scaling of the Source Dimensions of Interface and Intraslab Subduction-zone Earthquakes with Moment Magnitude. Seismological Research Letters 81, 941–950. https://doi.org/10.1785/gssrl.81.6.941

US EPA, O., 2014. EPANET [WWW Document]. URL https://www.epa.gov/water-research/epanet (accessed 4.10.23).

Xu, R., Jiang, R., Qu, T., 2021. Review of Dynamic Response of Buried Pipelines. J. Pipeline Syst. Eng. Pract. 12, 03120003. https://doi.org/10.1061/(ASCE)PS.1949-1204.0000527

Yoo, D.G., Kang, D., Kim, J.H., 2016. Optimal design of water supply networks for enhancing seismic reliability. Reliability Engineering & System Safety 146, 79–88. https://doi.org/10.1016/j.ress.2015.10.001

Yoon, S., Lee, Y.-J., Jung, H.-J., 2021. Flow-based seismic risk assessment of a water transmission network employing probabilistic seismic hazard analysis. Nat Hazards 105, 1231–1254. https://doi.org/10.1007/s11069-020-04352-7